Heterovibrational Interactions, Cooperative Hydrogen Bonding, and Vibrational Energy Relaxation Pathways in a Rotaxane

Bodis, P.; Timmer, R.; Yeremenko, S.; Buma, W.J.; Hannam, J.S.; Leigh, D.A.; Woutersen, S.

DOI
10.1021/jp070463s

Publication date
2007

Published in
The Journal of Physical Chemistry. C

Heterovibrational Interactions, Cooperative Hydrogen Bonding, and Vibrational Energy Relaxation Pathways in a Rotaxane

Pavol Bodis,[†,‡] Rutger Timmer,[‡] Sergey Yeremenko,[‡] Wybren Jan Buma,*[,†] Jeffrey S. Hannam,[§] David A. Leigh,*[,§] and Sander Woutersen*[,†,‡]

Van't Hoff Institute for Molecular Sciences, University of Amsterdam, Nieuwe Achtergracht 166, 1018 WV Amsterdam, The Netherlands, FOM Institute for Atomic and Molecular Physics, Kruislaan 407, 1098 SJ Amsterdam, The Netherlands, and School of Chemistry, University of Edinburgh, The King's Buildings, West Mains Road, Edinburgh EH9 3JJ, United Kingdom

Received: January 19, 2007; In Final Form: February 26, 2007

Femtosecond two-color vibrational pump−probe spectroscopy is used to investigate the interaction between the NH- and CO-stretch vibrations in a rotaxane composed of a benzylic amide macrocycle mechanically locked onto a succinamide-based thread. From the transient absorption spectrum, we obtain the cross anharmonicities and cross-peak anisotropies arising from the NH(macrocycle)/CO(macrocycle) and NH(macrocycle)/CO(thread) interactions. The cross-peak anisotropies are used to determine angles between NH and CO bonds in the macrocycle and the thread, providing structural information with picosecond temporal resolution. The CO and NH groups that form the macrocycle−thread hydrogen bonds are found to interact much more strongly than the CO and NH groups in other molecular systems containing the same NH···OC hydrogen-bond motif. We attribute this enhancement of the NH/CO anharmonic interaction to a cooperative effect, by which the two ring−thread hydrogen bonds sharing a hydrogen-bond acceptor mutually amplify each other. The relaxation dynamics of the NH/CO cross peaks has also been investigated. Surprisingly, the NH/CO cross peak observed upon exciting the NH-stretch mode decays much more slowly than the corresponding diagonal NH-stretch peak. This can be explained by the presence of an intermediate state that becomes populated in the NH-stretch vibrational relaxation and that is coupled to the CO-stretch mode. Our results demonstrate that NH/CO heterovibrational 2D-IR spectroscopy is well suited to observe the elementary hydrogen-bond making and breaking steps involved in the motion of rotaxane-based molecular devices.

I. Introduction

It has recently become possible to synthesize molecular assemblies that are capable of mechanical functions resembling those of machines.[1,2] At present, relatively little is known about the nature of the motions in such molecular systems. In particular, the dynamics of the noncovalent interactions that govern the movements of the connected components with respect to each other are generally only investigated on the NMR time scale (milliseconds to seconds). However, the component elementary motions necessarily involve interactions with molecules of the surrounding medium and take place on a picosecond time scale. Similar considerations apply to energy dissipation. The efficiency with which a molecular device can convert externally supplied energy into work is determined by competing relaxation processes, and many of these, in particular vibrational relaxation, take place on a picosecond time scale.[3,4]

Investigation of the motions of molecular devices requires time-resolved observation of working machines with ultrafast temporal resolution. The time-resolved structural probing required for this purpose can be achieved using the recently developed technique of two-dimensional infrared (2D-IR) spectroscopy.[5−10] 2D-IR Spectroscopy can be regarded as the optical analogue of 2D-NMR spectroscopy;[11] when two vibrations are coupled, this gives rise to cross peaks in the 2D-IR spectrum. From the intensity of these peaks, the coupling strength between the vibrations can be obtained.[6,7] Since the coupling is determined by the distance and orientation of the coupled vibrating bonds,[12−16] a 2D-IR spectrum gives structural information analogous to that of 2D-NMR (where couplings between spins are used for the same purpose[11]) but with a time resolution on the order of a picosecond (determined by the pulse duration and the free-induction decay of the vibrational transition). In addition, 2D-IR also gives information about the vibrational relaxation; from the time dependence of the diagonal peaks, the decay of the vibrational excitation can be directly monitored, again with picosecond temporal resolution.

Rotaxanes and catenanes[17] are often thought of as potential building blocks for molecular devices.[1,2] In amide-based systems,[18] their operation as machines involves the making and breaking of NH···OC hydrogen bonds between the constituent components.[19] When there is more than one hydrogen-bonding site, externally induced changes in the hydrogen-bond affinities can be used to move the components with respect to each other in a controlled way, an effect that has been used to construct rotaxane-based molecular shuttles,[19] motors,[20,21] and ratchets.[22] Couplings between the vibrations of the NH and CO bonds that are involved in the intercomponent hydrogen bonds should be very sensitive to the instantaneous structure of rotaxane devices and, therefore, ideally suited for studying their motions in time-resolved 2D-IR experiments. Such couplings between different

* To whom correspondence should be addressed. E-mail: w.j.buma@uva.nl (W.J.B), david.leigh@ed.ac.uk (D.A.L.), s.woutersen@uva.nl (S.W.).
[†] University of Amsterdam.
[‡] FOM Institute for Atomic and Molecular Physics.
[§] University of Edinburgh.

10.1021/jp070463s CCC: $37.00
Published on Web 04/07/2007

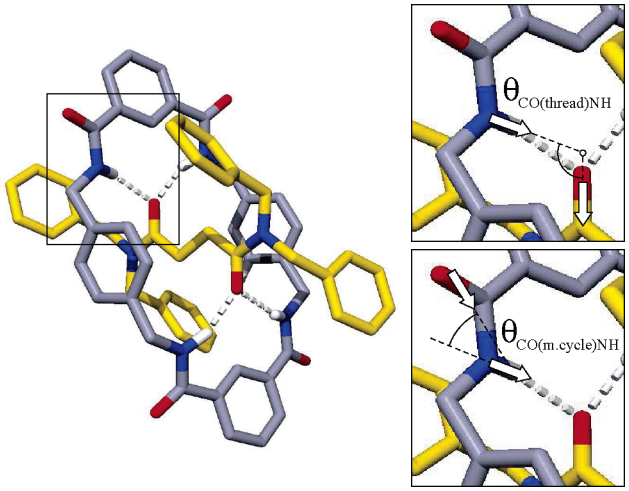

Figure 1. X-ray structure[31] of the [2]rotaxane investigated in this study. The insets show the angles $\theta_{CO(thread)-NH}$ and $\theta_{CO(m.cycle)-NH}$ that have been determined from the NH/CO(thread) and NH/CO(m.cycle) cross anisotropies; see Section III.D.2. In the amide group, there is an angle of ~20° between the CO-stretch transition dipole and the C=O bond.[12]

types of vibrating chemical bonds can be regarded as the vibrational analogue of heteronuclear couplings in NMR.[11,16,23] NH/CO Heterovibrational couplings have previously been measured in dipeptides[24] and small organic molecules.[25] These NH/CO couplings are of general physical and chemical importance, as they occur not only in rotaxanes but also in base-paired DNA and in peptides.[24,26] In each of these systems, the values of the NH/CO coupling strength is directly related to the molecular conformation.

Here, we show how NH/CO heterovibrational couplings can be used to probe the co-conformation[27] of rotaxane-based devices. The time resolution of the structural probing is on the order of a picosecond (determined by the convolution of the free-induction decay with the pulse duration), which makes the observation of fast molecular motions possible.[28] Here, we do not yet report on such motions but will focus on the relationship between the observed vibrational couplings and the molecular conformation. We use two-color IR pump−probe spectroscopy to study a [2]rotaxane consisting of a benzylic amide macrocycle mechanically locked onto a succinamide-based thread and held in position by a network of four NH···OC hydrogen bonds (see Figure 1). This rotaxane, of which we previously investigated the CO/CO ("homovibrational") interactions,[29,30] is representative of a large class of rotaxane- and catenane-based devices that includes molecular shuttles and motors.[19] We also investigate the relaxation dynamics of the NH- and CO-stretch modes and of the NH/CO cross peaks. Apart from the importance of vibrational relaxation in determining the energy conversion efficiency of molecular devices, knowledge of the relaxation rates and pathways is essential for the interpretation of heterovibrational 2D-IR spectra since different T_1 lifetimes of coupled modes may give rise to apparent delay dependences of the observed couplings.

II. Materials and Methods

Two types of experiments have been performed, one-color experiments, in which the same vibrational mode (either NH- or CO-stretch) is pumped and probed, and two-color experiments, in which the NH-stretch mode is excited and the CO-stretch modes are probed. The setup employed in the one-color experiments is based on the design reported by Hamm et al.[32] An optical parametrical amplifier (OPA) based on BBO is pumped by a commercial Ti:sapphire laser system (Spectra-Physics Hurricane, 1 mJ, 100 fs). To excite the CO-stretch modes, the output of the OPA (energy of signal + idler ~ 100 μJ) is used to generate mid-IR pulses using difference-frequency generation of signal and idler in $AgGaS_2$. The resulting mid-IR pulses at 1650 cm^{-1} have a duration of ~200 fs, an energy of 1 μJ, and a bandwidth of ~150 cm^{-1} (fwhm). To excite the NH-stretch mode, the BBO-doubled idler from the OPA is mixed in KTP with 200 μJ of residual 800 nm light from the Hurricane. The resulting mid-IR pump pulses at 3450 cm^{-1} have a duration of ~100 fs, an energy of 10 μJ, and a bandwidth of ~200 cm^{-1} (fwhm). In the two-color experiments, we use a setup consisting of two OPAs based on BBO that are pumped by a commercial Ti:sapphire laser system (Quantronix Titan, 2.4 mJ, 100 fs). Using the same approach as above to generate 3 and 6 μm, we obtain 15 μJ light at 3450 cm^{-1} (150 fs, fwhm ~ 100 cm^{-1}) and 1 μJ at 1650 cm^{-1} (200 fs, fwhm ~ 200 cm^{-1}).

The probe and reference pulses are obtained from the generated IR light by reflection from the surfaces of a wedged BaF_2 window. The pump and probe pulses are focused and overlapped in the sample by means of an $f = 100$ mm off-axis parabolic mirror (focal diameters of ~400 and ~250 mm for pump and probe, respectively), and transient absorption changes are measured by frequency-dispersed detection of probe and reference pulses using a 2 × 32 HgCdTe array detector. The polarizations of the pump and probe pulses are set either parallel or perpendicular with respect to each other by means of a zero-order half-wave plate. The time response of both experimental setups is determined from cross-correlation experiments in CaF_2.

The synthesis and purification of the rotaxane have been described in detail elsewhere.[31] All experiments are carried out at room temperature on a 2.5 mM solution of the rotaxane in $CDCl_3$. To remove traces of water from the $CDCl_3$, it is distilled at atmospheric pressure, and the rotaxane solution is prepared under an Ar atmosphere. The sample is kept in a sealed cell consisting of two CaF_2 windows separated by a 1 mm spacer. We observe a nonresonant response (mainly from the solvent) at delays where the pump and probe pulse are temporally overlapped. To ensure that these nonresonant effects do not influence the quantitative interpretation, all data analysis is done starting from delay values (400 fs for the NH-pump/NH-probe; 700 fs for the other experiments) at which the nonresonant contribution has become negligible compared to the resonant signal. In some of the measurements, a small thermal contribution to the signal is observed at long pump−probe delays. This thermal signal is due to a small increase in the temperature of the sample after vibrational relaxation (at most 0.1 K, as estimated from the focal diameter and pulse energy). In the least-squares fitting of the data, this thermal contribution is assumed to grow in with the rate of the vibrational relaxation.

III. Results and Discussion

A. General Considerations. Figure 2 shows the steady-state absorption spectrum of the [2]rotaxane in $CDCl_3$. The peaks at 1610 and 1660 cm^{-1} are due to the CO-stretch modes of the thread and the amide I mode of the macrocycle, respectively.[29] The peak at 3370 cm^{-1} is due to the amide A mode of the macrocycle (the thread does not contain any NH groups). As the amide I mode involves mainly the stretching of the CO bond and the amide A mode mainly that of the NH bond, in the following, these modes will simply be referred to as CO- and NH-stretch modes, respectively. Because of the symmetry of the rotaxane, the two CO groups in the thread are equivalent, and the same holds for the four CO groups and four NH groups

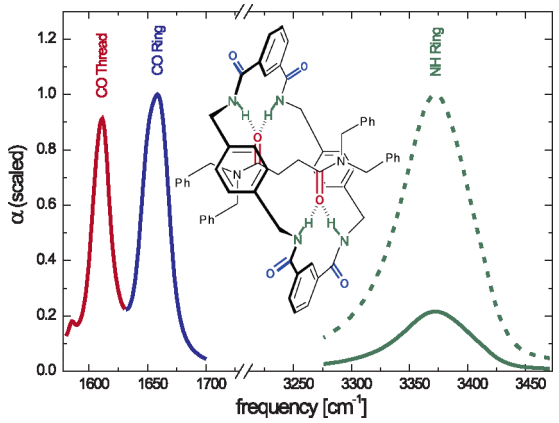

Figure 2. Infrared absorption spectrum of a 2.5 mM solution of the investigated [2]rotaxane in $CDCl_3$. The colors of the peaks match those of the highlighted bonds in the chemical structure. The dotted curve represents the NH-stretch absorption multiplied by a factor of 5.

in the macrocycle. The amplitude of the peaks of the CO-stretch modes is much larger than that of the NH-stretch modes, but the frequency-integrated absorption cross sections are comparable since the fwhm of the NH-stretch band is larger by approximately the same factor. In all experiments, the power spectrum of the excitation pulse is much broader than the widths of the absorption bands that are resonantly excited. Hence, spectral diffusion is not observable in the experiments. In the following, we first discuss the relaxation dynamics of the NH- and CO-stretch modes (Sections III.B and III.C) before describing the NH/CO interactions (Section III.D).

B. NH-Stretch Mode. The linear and the transient absorption spectra for parallel and perpendicular polarizations of the pump and probe beams are shown in Figure 3a. From the ratio of the parallel and perpendicular signals, we find an anisotropy of 0.36, close to the theoretically expected value of 0.4. From the transient spectra, we can determine the diagonal anharmonicity (difference between the $v = 0 \rightarrow 1$ and $v = 1 \rightarrow 2$ transition frequencies) of the NH-stretch mode. Since the power spectrum of the excitation pulse is much broader than the NH-stretch absorption band $\alpha_0(\nu)$, the entire absorption band is excited simultaneously. As a consequence, spectral diffusion is not observable, and the absorption change due to ground-state bleaching and stimulated emission can be well described by a negative contribution with the shape of the steady-state absorption spectrum $\alpha_0(\nu)$. We assume that the $v = 1 \rightarrow 2$ line shape is similar to the $v = 0 \rightarrow 1$ line shape but allow for a difference in width (to account for faster dephasing of the $v = 1 \rightarrow 2$ transition as compared to the $v = 0 \rightarrow 1$ transition, for instance, as a consequence of faster vibrational relaxation of the $v = 2$ state) and an intensity scaling factor (to allow a deviation from the harmonic approximation in which this scaling factor would be unity[33]). Using a Gaussian to describe $\alpha_0(\nu)$, this simple approach provides a good description of the observed $\Delta\alpha(\nu)$ (see Figure 3a). From a least-squares fit to the data at 1 ps delay, we obtain a value of 153 ± 4 cm^{-1} for the NH-stretch anharmonicity, similar to the values reported elsewhere for the diagonal anharmonicities of the NH-stretch (amide A) mode of amide groups in peptides.[24,26]

Figure 3b shows the transient absorption change as a function of delay between the pump and probe pulses for several probing frequencies. We find that the delay dependence can be well described by a single-exponential decay, and from a simultaneous least-squares fit to the delay-dependent absorption changes at all probing frequencies (using the same time constant for all frequencies), we find an excited-state lifetime T_1 of 2.24 ± 0.12

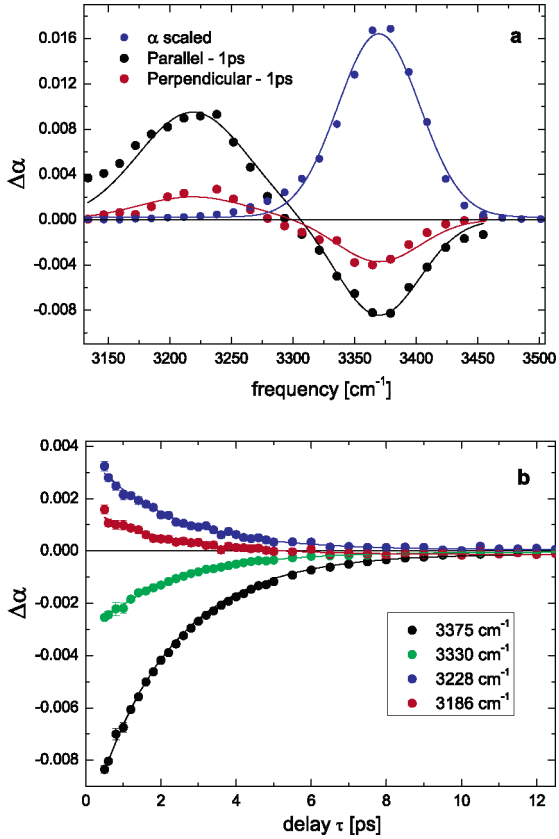

Figure 3. (a) Linear and transient absorption spectra for parallel and perpendicular polarization of the probe with respect to the pump. The solid lines are least-squares fits using a Gaussian function to describe the absorption band. (b) Transient absorption change of the NH-stretch mode as a function of delay between the pump and probe pulse for several representative probing frequencies. The solid lines are least-squares fits to single-exponential decays.

ps. The observed lifetime is significantly longer than the 0.58 ps observed for the dipeptide acetyl proline−OMe in chloroform.[24] In chloroform, acetyl proline−OMe is in the C_7 conformation, which contains an internal NH···OC hydrogen bond, leading to a red-shifted NH-stretch frequency of 3333 cm^{-1}. This NH-stretch frequency is lower than that of the rotaxane (3370 cm^{-1}), which implies that the hydrogen bonding in the dipeptide is stronger than in the rotaxane. The stronger hydrogen bonding probably explains the faster vibrational relaxation in the peptide as compared to the rotaxane, as stronger hydrogen bonding generally increases the rate of vibrational relaxation.[34]

C. CO-Stretch Modes. Figure 4a shows the transient absorption change upon exciting the CO-stretch region (the spectrum of the pump pulse covers both the thread and macrocycle CO-stretch modes). The spectrum can be quantitatively analyzed in the same way as the NH-stretch mode; the absorption bands of the thread and macrocycle CO-stretching modes are each modeled by a Gaussian, and the transient absorption spectrum of each mode as the sum of a bleaching/stimulated-emission part identical to the absorption band and a red-shifted induced absorption, which is modeled as a Gaussian. From a least-squares fit, we find diagonal anharmonicities of 10 ± 3 and 5 ± 3 cm^{-1} for the thread and macrocycle CO-stretch modes, respectively, in agreement with the estimate from the 2D-IR spectrum.[29] To investigate if energy transfer between the CO-stretch modes occurs,[35] we have also performed experiments in which either the thread or the macrocycle CO-stretch mode is selectively pumped with a narrow-band pump pulse

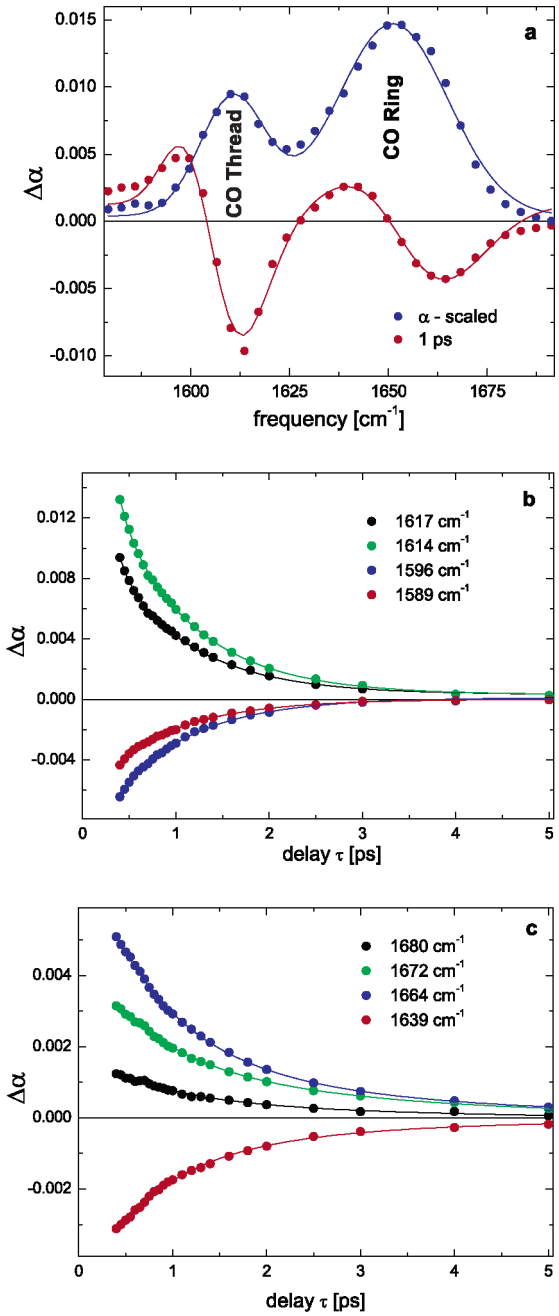

Figure 4. (a) Linear (blue points) and transient absorption spectra at a delay of 1 ps (red points) showing the frequency region containing the CO-stretch modes of the thread (1610 cm^{-1}) and the macrocycle (1655 cm^{-1}). The solid lines are the result of least-squares fits assuming Gaussians for the line shapes. (b) Transient absorption change of the thread CO-stretch mode as a function of delay between the pump and probe pulse for several representative probing frequencies. The solid lines are simultaneous least-squares fits of a single-exponential decay. (c) The same as (b) for the CO-stretch mode of the macrocycle.

(fwhm 13 cm^{-1}), and both modes are probed. We then observe decays with the respective T_1's at the tread or macrocycle mode but no significant energy transfer between the modes. The delay dependence of the absorption change is shown in Figure 4b,c. From simultaneous least-squares fits of exponential decays for the CO-stretch modes of the thread and of the macrocycle, we find T_1 values of 0.79 ± 0.12 and 0.96 ± 0.07 ps, respectively.

D. NH−CO Interactions. *1. Cross Anharmonicities.* The response of the CO-stretch modes upon excitation of the NH-stretch mode is shown in Figure 5a together with the NH-stretch response. This graph can be regarded as a cross section through

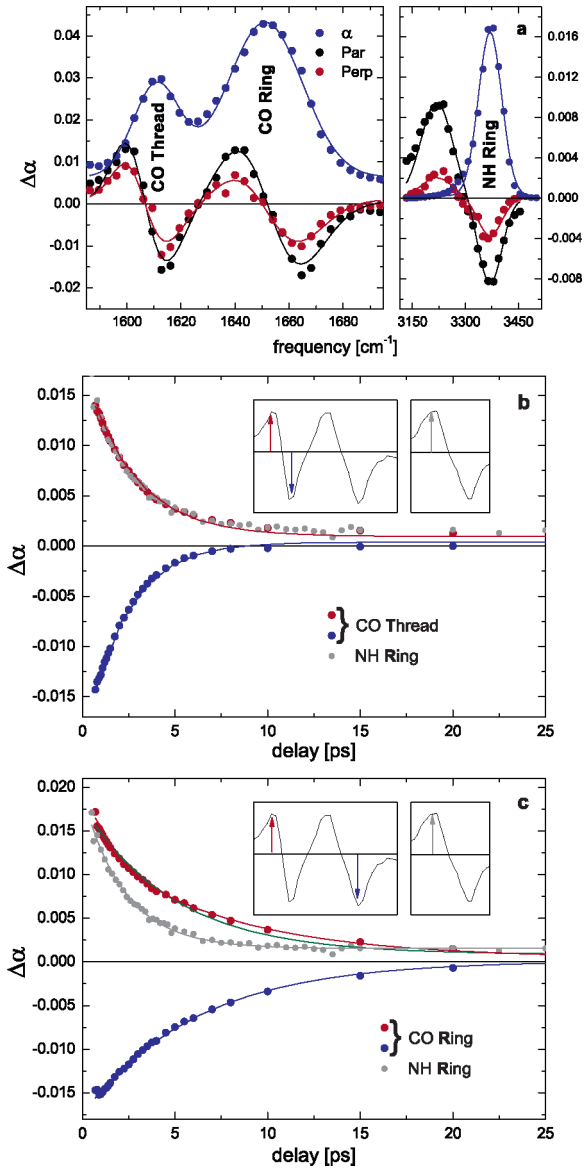

Figure 5. (a) Linear (blue points) and transient absorption change (red and black points) upon exciting the NH-stretch mode. The solid black and red lines show the pump−probe spectrum at 1 ps delay for parallel and perpendicular polarization, respectively. (b) Delay dependence of the thread CO-stretch response at 1599 (red points) and 1613 cm^{-1} (blue points) and of the NH-stretch response at 3242 cm^{-1} (gray points). The probing frequencies are indicated by arrows in the inset. (c) Delay dependence of the CO-stretch response of the macrocycle at 1640 (red points) and 1665 cm^{-1} (blue points) and of the NH-stretch response at 3242 cm^{-1} (gray points). The green curve shows a single-exponential fit to the CO-stretch data; the red and blue curves are double-exponential fits.

a two-dimensional IR spectrum, where the NH-response is the diagonal peak and the positive−negative doublets in the CO-stretch region are cross peaks. For both CO-stretch modes, the signal rises instantaneously (within the system response of ~250 fs). This implies that no energy transfer from the NH-stretch to either of the CO-stretch modes takes place since such energy transfer would imply an ingrowth of the CO-stretch signal with a time constant equal to the ~2.2 ps lifetime of the NH-stretch mode. Hence, the NH−CO cross peaks must be due to coupling between the NH- and CO-stretch modes. From the shape and amplitude of each of the two CO-stretch cross peaks, the corresponding cross anharmonicity (the difference between the frequency of the $|v_{NH} = 1, v_{CO} = 0\rangle \rightarrow |v_{NH} = 1, v_{CO} = 1\rangle$ and $|v_{NH} = 0, v_{CO} = 0\rangle \rightarrow |v_{NH} = 0, v_{CO} = 1\rangle$ transitions) can be

determined,[6,36] as well as the cross-peak anisotropy (dependence on the relative polarization of pump and probe).[6] The latter is defined for two coupled vibrations, i and j, as[6]

$$R_{ij} = \frac{\Delta\alpha_{ij}^{||} - \Delta\alpha_{ij}^{\perp}}{\Delta\alpha_{ij}^{||} + 2\Delta\alpha_{ij}^{\perp}}$$

where $\Delta\alpha_{ij}^{||}$ and $\Delta\alpha_{ij}^{\perp}$ are the cross-peak intensities for parallel and perpendicular polarizations of the pump and probe pulses. The shape of each cross peak can be described as the sum of a negative part caused by the bleaching of the common vibrational ground state upon excitation of the NH-stretch mode and a positive part due to the induced absorption from the $|v_{NH} = 1, v_{CO} = 0\rangle$ to the $|v_{NH} = 1, v_{CO} = 1\rangle$ state (which occurs at a frequency lower than the fundamental $|v_{NH} = 0, v_{CO} = 0\rangle \rightarrow |v_{NH} = 0, v_{CO} = 1\rangle$ transition)

$$\Delta\alpha_{cross}(\nu) = -\alpha_0(\nu) + \alpha_0(\nu + \Delta_{CO-NH}) \qquad (1)$$

where it is assumed that the CO-stretch line shape $\alpha_0(\nu)$ does not change upon excitation of the NH-stretch mode. We model each of the two cross peaks (for the macrocycle and thread CO-stretch modes) by the above expression using Gaussians for $\alpha_{0,thread}(\nu)$ and $\alpha_{0,m.cycle}(\nu)$, which we obtain from a least-squares fit to the steady-state absorption spectrum. Fitting this model to the CO-stretch transient spectrum, treating the two cross anharmonicities $\Delta_{CO(thread)-NH}$ and $\Delta_{CO(m.cycle)-NH}$ and the cross-peak anisotropies as free parameters, we obtain the fit shown as the solid curves in Figure 5a. From this fit, we obtain $\Delta_{CO(thread)-NH} = 9.5 \pm 2.2\ cm^{-1}$ and $\Delta_{CO(m.cycle)-NH} = 5.1 \pm 2.4\ cm^{-1}$ for the cross anharmonicities and $R_{CO(thread)-NH} = 0.15 \pm 0.03$ and $R_{CO(m.cycle)-NH} = 0.22 \pm 0.04$.

The cross anharmonicity between the NH-stretch and $CO_{m.cycle}$-stretch mode is essentially a property of the amide group and should, therefore, be comparable to the cross anharmonicity observed between the NH-stretch (amide A) and CO-stretch (amide I) modes of the amide group in acetyl proline−OMe in chloroform. For the latter, a value of $3.5 \pm 0.3\ cm^{-1}$ is observed,[24] slightly less than the $5.1 \pm 2.4\ cm^{-1}$ observed here. The larger cross anharmonicity in the rotaxane is probably due to the presence of double hydrogen bonds in this molecule; see below.

The $\Delta_{CO(thread)-NH}$ cross anharmonicity arises from interaction between the macrocycle NH and thread CO groups across the hydrogen bond connecting them. Although this interaction is very sensitive to the strength and direction of the NH···OC hydrogen bond, a quantitative interpretation of the observed cross anharmonicity in terms of specific conformational parameters requires detailed quantum chemical modeling of the influence of hydrogen bonding on the cross anharmonicity. At present, theoretical work in this direction is actively being pursued.[15,37,38]

It is interesting to compare the value of $9.5 \pm 2.2\ cm^{-1}$ observed for the NH/CO_{thread} cross anharmonicity to that between the hydrogen-bonded NH and CO groups in the peptide acetyl proline−OMe. In chloroform, this peptide adapts the C_7 conformation and contains an internal NH···OC hydrogen bond.[24] Both in the peptide and in the rotaxane, the NH/CO cross anharmonicity arises mainly from through-hydrogen-bond effects. In the peptide, the NH-stretch frequency is lower than that in the rotaxane (3333 vs 3370 cm^{-1}), which implies that the NH···OC hydrogen bond is stronger in the peptide than in the rotaxane.[39] One would therefore expect a stronger NH/CO anharmonic interaction in the peptide and hence a higher NH/CO cross anharmonicity. Surprisingly, the exact opposite is observed; the cross anharmonicity of the CO and NH groups connected by the hydrogen bond is much smaller in the peptide ($1.4 \pm 0.4 cm^{-1}$)[24] than in the rotaxane ($9.5 \pm 2.2 cm^{-1}$). We believe that the stronger anharmonic interaction between the NH- and CO-stretch modes observed in the rotaxane is most probably due to a cooperative effect[39] of the two NH···OC hydrogen bonds coordinated to the same CO group (see Figure 1). Each NH···OC hydrogen bond-polarizes the charges of the CO group, and this polarization of the CO group enhances the anharmonic NH/CO interaction through the other NH·····OC hydrogen bond. Hence, even though the individual hydrogen bonds are weaker in the rotaxane than in the peptide, the cooperative effect of a double hydrogen bond to the same acceptor leads to an amplification of the anharmonic NH/CO interaction, giving rise to the larger NH/CO cross anharmonicity in the rotaxane. This enhancement of anharmonic interactions should occur in all doubly-hydrogen-bonded systems, notably in DNA and protein structures. In DNA, the CO groups of the nucleotides simultaneously form hydrogen bonds to the NH groups of the complementary bases and to the OH groups of the solvating water.[40,41] In alpha helices, the amide CO groups simultaneously hydrogen bond to amide NH groups and the solvating water.[42] Our measurements suggest that rotaxanes might be suitable model systems for studying hydrogen-bond cooperativity in these more complicated and heterogeneous biochemical structures since the hydrogen-bond geometry in rotaxanes is well defined.

2. Cross Anisotropies and Structural Information. The cross-peak anisotropies R_{ij} are directly related to the angle θ_{ij} between the transition-dipole moments of the coupled vibrations[6]

$$R_{ij} = (3\cos^2\theta_{ij} - 1)/5 \qquad (2)$$

From the cross anisotropies $R_{CO(thread)-NH} = 0.15 \pm 0.03$ and $R_{CO(m.cycle)-NH} = 0.22 \pm 0.04$, we obtain angles $\theta_{CO(thread)-NH} = 139 \pm 3°$ and $\theta_{CO(m.cycle)-NH} = 33°$ (see Figure 1 for the definition of the angles). The angle of $33 \pm 4°$ between the NH- and CO-stretch mode transition dipoles of the amide group of the macrocycle is very similar to the value of $34.5 \pm 3°$ found for this angle in the amide group of acetyl proline−OMe,[24] a peptide in which the amide group forms an internal NH···OC hydrogen bond (in non-hydrogen-bonded peptides, a smaller value of $23 \pm 3°$ is found[43]). The similarity of the dipole−dipole angles in the rotaxane and in the hydrogen-bond-containing peptide suggests that the value of this angle is determined mainly by the presence (and strength) of a hydrogen bond, independent of whether the amide group is in a peptide or in a rotaxane. Assuming an angle of 20° between the amide I transition dipole and the C═O bond,[12] we obtain an angle $\angle(N-H, C{=}O_{m.cycle})$ of ~15°, close to the value of 12° in the X-ray structure.[31,44]

The angle between the NH-stretch mode of the macrocycle and the CO-stretch mode of the thread is directly related to the relative position and orientation of the two rotaxane components. Assuming that the CO-stretch transition dipole is parallel to the C═O bond and the NH-stretch transition dipole is parallel to the N−H bond,[12] we predict an angle $\angle(N-H, C{=}O_{thread})$ (indicated in Figure 1) of 139° from the observed cross-peak anisotropy. This value again agrees fairly well with the angle in the X-ray structure,[31] which is $\angle(N-H, C{=}O_{thread}) = 114°$.[44] The discrepancy may be due to a difference between the solution and X-ray structures but could also be due to a small angle between the thread C═O bond and the CO-stretch transition-dipole moment. It may be noted that, although both the cross

anharmonicity and the cross anisotropy are sensitive probes of the rotaxane co-conformation, unlike the cross anharmonicity, the cross anisotropy can be used in a straightforward manner to obtain quantitative information (notably the angles indicated in Figure 1) about the relative orientation of the macrocycle and the thread.

3. NH−CO Cross-Peak Dynamics. We have studied the cross-peak relaxation dynamics in the rotaxane by measuring two-color pump−probe spectra as a function of delay. In these experiments, the NH-stretch mode is excited, and the dynamics of the CO-stretch modes is probed. The result for the CO_{thread}-stretch mode of the thread is shown in Figure 5b. From a least-squares fit (solid lines in Figure 5b), we find that the decay of the CO_{thread}-stretch response occurs with a time constant of 2.36 ± 0.15 ps (and a very small component with a time constant of 18 ± 4 ps). This decay exactly matches that of the $v = 1$ population of the NH-stretch mode ($T_1 = 2.24 \pm 0.12$ ps), as can be seen from the gray curve which represents the decay of the NH-stretch excited-state absorption. Together with the instantaneous ingrowth of the CO-stretch signal, this implies that the NH−CO_{thread} cross peak is caused purely by a coupling between the NH-stretch mode and the CO_{thread}-stretch mode and involves no other modes; the cross peak vanishes together with the $v = 1$ population of the NH-stretch mode.

Interestingly, in case of the macrocycle CO-stretch mode, the decay of the cross-peak intensity is much slower than that of the NH-stretch excited-state population; see Figure 5c. From a simultaneous biexponential least-squares fit, we find decay constants of 2.4 ± 0.2 and 7.2 ± 0.12 ps, respectively, with comparable amplitudes for the two components. The data cannot be described by a single-exponential decay (green curve in Figure 5c). Apparently, the CO-stretch mode of the macrocycle is coupled not only to the NH-stretch mode but also to another mode, which we will refer to as X. Since a coupling between the macrocycle CO-stretch mode and mode X is observed after excitation of the NH-stretch mode, we can conclude that mode X acts as an accepting mode in the energy relaxation of the NH-stretch mode; see Figure 6. A similar phenomenon has been observed in the cross-peak dynamics of peptides.[24] The relaxation of the NH-stretch mode involves a transfer of the vibrational energy to mode X, which acts as an intermediate state in the vibrational relaxation process. The excited-state of mode X is thus populated with a time constant equal to the T_1 of the NH-stretch mode, and it subsequently relaxes with a time constant τ. The $CO_{m.cycle}$-stretch mode is coupled to both the NH-stretch mode and to mode X, and hence, the delay dependence of the cross-peak intensity is governed by both time constants T_1 and τ.[24] Assuming that the population relaxation of both the NH-stretch mode and mode X occurs in a single-exponential manner, the excited-state populations of the NH-stretch mode and mode X can be easily shown to be given by

$$n_{|10\rangle}(t) = e^{-t/T_1} \tag{3}$$

$$n_{|00X\rangle}(t) = \frac{T_1^{-1}}{T_1^{-1} - \tau^{-1}}\left(e^{-t/\tau} - e^{-t/T_1}\right) \tag{4}$$

where the labeling of the states is as in Figure 6. The NH−$CO_{m.cycle}$ cross peak is due to two contributions, (i) a coupling between the $CO_{m.cycle}$-stretch and the NH-stretch mode and (ii) a coupling between the $CO_{m.cycle}$-stretch and the accepting mode X. The delay-dependent cross-peak intensity is then given by

$$I_{NH-CO}(t) = \Delta_{NH-CO} \cdot n_{|10\rangle}(t) + \Delta_{X-CO} \cdot n_{|00X\rangle}(t) \tag{5}$$

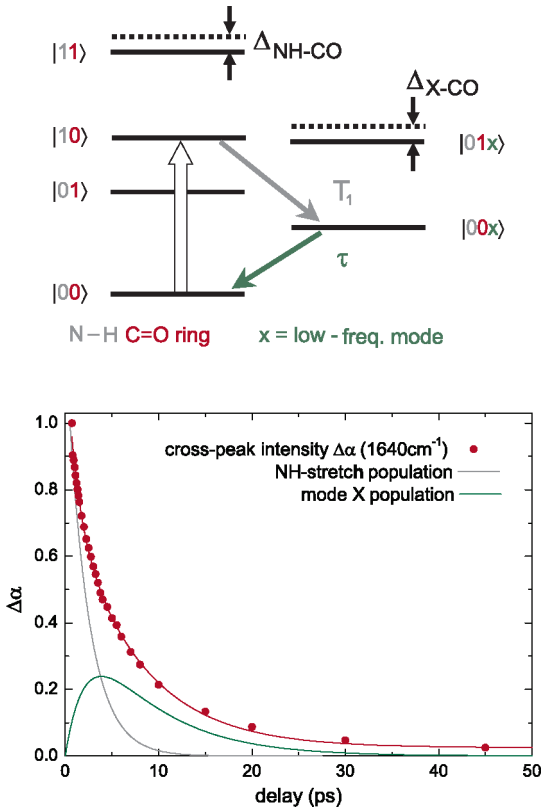

Figure 6. Top: energy level diagram illustrating the effect of the vibrational relaxation of the NH-stretch mode on the CO-stretch mode of the macrocycle ring. Bottom: delay dependence of the NH−$CO_{m.cycle}$ cross-peak intensity (red points) and a least-squares fit of eq 5 to the data (red curve). The excited-state populations of the NH-stretch mode and the accepting mode X are shown as the gray and green curves, respectively.

where Δ_{NH-CO} is the NH−CO cross anharmonicity and Δ_{X-CO} the X−CO cross anharmonicity. Fitting this expression to the observed decay of the cross-peak intensity (with the ratio $\Delta_{X-CO}/\Delta_{NH-CO}$ and an overall scaling factor as the free parameters), we obtain $\Delta_{X-CO}/\Delta_{NH-CO} = 0.40 \pm 0.01$, which implies that the CO-stretch mode interacts more strongly with the NH-stretch mode than with the accepting mode X. The result of the fit and the corresponding populations $n_{|10\rangle}(t)$ and $n_{|00X\rangle}(t)$ are shown in Figure 6. From this graph, it can be seen that, at short pump−probe delays, the cross-peak intensity mainly represents the coupling between the CO and the NH modes, whereas at delays beyond ~4 ps, it represents mainly the coupling between the CO and the X mode. This result clearly illustrates the importance of detailed knowledge of the relaxation dynamics for the interpretation of heterovibrational 2D-IR spectra.

IV. Conclusions

We have shown that heterovibrational 2D-IR spectroscopy can be used to probe the co-conformation of a rotaxane with picosecond time resolution. In particular, the angles between the NH and CO groups in the macrocycle and thread, indicated in Figure 1, have been determined directly from the NH/CO cross-peak anisotropies. The cross anharmonicities are found to exhibit a similar sensitivity to the rotaxane co-conformation, and the observed large NH/CO_{thread} cross anharmonicity suggests cooperativity of the macrocycle−thread hydrogen bonding.

Although 2D-IR experiments on moving molecular devices have not yet been performed, our results clearly demonstrate the feasibility of time-resolved dual-frequency 2D-IR experi-

ments in which externally triggered structural changes of molecular machines are measured with picosecond time resolution. By monitoring the appearance and disappearance of specific NH/CO cross peaks, the hydrogen-bond making and breaking at specific hydrogen-bonding sites of a molecular device can be observed separately and in real time, leading to a detailed picture of the device motion. We believe this will lead to insights into the functioning of molecular devices that are difficult to obtain with other experimental methods.

Acknowledgment. We gratefully acknowledge Hinco Schoenmaker for technical support and Mischa Bonn for critically reading the manuscript. This work has been partly financed by the European Community (EMMMA (HPRN-CT-2002-00168) and Hy3M (NMP-CT-2004-013525) networks) and is part of the research program of the "Stichting voor Fundamenteel Onderzoek der Materie (FOM)", which is financially supported by the "Nederlandse organisatie voor Wetenschappelijk Onderzoek (NWO)".

References and Notes

(1) For recent reviews, see: (a) Balzani, V.; Venturi, M.; Credi, A. *Molecular Devices and Machines*. *A Journey into the Nanoworld*; Wiley-VCH: Weinheim, Germany, 2003. (b) Flood, A. H.; Ramirez, R. J. A.; Deng, W. Q.; Muller, R. P.; Goddard, W. A.; Stoddart, J. F. *Aust. J. Chem.* **2004**, *57*, 301. (c) Kay, E. R.; Leigh, D. A. In *Functional Artificial Receptors*; Schrader, T., Hamilton, A. D., Eds.; Wiley-VCH: Weinheim, Germany, 2005; pp 333−406.

(2) For recent examples, see: (a) Balzani, V.; Credi, A.; Silvi, S.; Stoddart, J. F. *Science* **2004**, *303*, 1845. (b) Fletcher, S. P.; Dumur, F.; Pollard, M. M.; Feringa, B. L. *Science* **2005**, *310*, 80. (c) Bern, J.; Leigh, D. A.; Lubomska, M.; Mendoza, S. M.; Pérez, E. M.; Rudolf, P.; Teobaldi, G.; Zerbetto, F. *Nature Mater.* **2005**, *4*, 70. (d) Nguyen, T. D.; Tseng, H.-R.; Celestre, P. C.; Flood, A. H.; Liu, Y.; Stoddart, J. F.; Zink, J. I. *Proc. Natl. Acad. Sci. U.S.A.* **2005**, *102*, 10029. (e) Eelkema, R.; Pollard, M. M.; Vicario, J.; Katsonis, N.; Serrano Ramon, B.; Bastiaansen, C. W. M.; Broer, D. J.; Feringa, B. L. *Nature* **2006**, *440*, 163.

(3) Oxtoby, D. W. *Adv. Chem. Phys.* **1981**, *47*, 487.

(4) Owrutski, J. C.; Raftery, D.; Hochstrasser, R. M. *Annu. Rev. Phys. Chem.* **1994**, *45*, 519.

(5) Zhang, W. M.; Chernyak, V.; Mukamel, S. *J. Chem. Phys.* **1999**, *110*, 5011.

(6) Hamm, P.; Lim, M.; DeGrado, W. F.; Hochstrasser, R. M. *Proc. Natl. Acad. Sci. U.S.A.* **1999**, *96*, 2036.

(7) Golonzka, O.; Khalil, M.; Demirdöven, N.; Tokmakoff, A. *Phys. Rev. Lett.* **2001**, *86*, 2154.

(8) Jonas, D. M. *Science* **2003**, *300*, 1515.

(9) Stolow, A.; Jonas, D. M. *Science* **2004**, *305*, 1575.

(10) Zanni, M. T.; Ge, N. H.; Kim, Y. S.; Hochstrasser, R. M. *Proc. Natl. Acad. Sci. U.S.A.* **2001**, *98*, 11265.

(11) Ernst, R. R.; Bodenhausen, G.; Wokaun, A. *Principles of Nuclear Magnetic Resonance in One and Two Dimensions*; Clarendon Press: Oxford, U.K., 1987.

(12) Krimm, S.; Bandekar, J. *Adv. Protein Chem.* **1986**, *38*, 181.

(13) Torii, H.; Tasumi, M. *J. Raman Spectrosc.* **1998**, *29*, 81.

(14) Cheatum, C. M.; Tokmakoff, A.; Knoester, J. *J. Chem. Phys.* **2004**, *120*, 8201.

(15) Moran, A.; Mukamel, S. *Proc. Natl. Acad. Sci. U.S.A.* **2004**, *101*, 506.

(16) Scheurer, C.; Mukamel, S. *J. Chem. Phys.* **2002**, *116*, 6803.

(17) Sauvage, J.-P., Dietrich-Bucheker, C., Eds. *Molecular Catenanes, Rotaxanes and Knots*; Wiley-VCH: Weinheim, Germany, 1999.

(18) Kay, E. R.; Leigh, D. A. *Top. Curr. Chem.* **2005**, *262*, 133.

(19) (a) Brouwer, A. M.; Frochot, C.; Gatti, F. G.; Leigh, D. A.; Mottier, L.; Paolucci, F.; Roffia, S.; Wurpel, G. W. H. *Science* **2001**, *291*, 2124. (b) Leigh, D. A.; Wong, J. K. Y.; Dehez, F.; Zerbetto, F. *Nature* **2003**, *424*, 174. (c) Leigh, D. A.; Morales, M. A. F.; Pérez, E. M.; Wong, J. K. Y.; Saiz, C. G.; Slawin, A. M. Z.; Carmichael, A. J.; Haddleton, D. M.; Brouwer, A. M.; Buma, W. J.; Wurpel, G. W. H.; León, S.; Zerbetto, F. *Angew. Chem., Int. Ed.* **2005**, *44*, 3062. (d) Marlin, D. S.; González Cabrera, D.; Leigh, D. A.; Slawin, A. M. Z. *Angew. Chem., Int. Ed.* **2006**, *45*, 1385.

(20) Leigh, D. A.; Wong, J. K. Y.; Dehez, F.; Zerbetto, F. *Nature* **2003**, *424*, 174.

(21) Hernandez, J. V.; Kay, E. R.; Leigh, D. A. *Science* **2004**, *306*, 1532.

(22) Serreli, V.; Lee, C.-F.; Kay, E. R.; Leigh, D. A. *Nature* **2007**, *445*, 523.

(23) Scheurer, C.; Mukamel, S. *J. Chem. Phys.* **2001**, *115*, 4989.

(24) Rubtsov, I. V.; Wang, J.; Hochstrasser, R. M. *J. Phys. Chem. A* **2003**, *107*, 3384.

(25) Kurochkin, D. V.; Naraharisetty, S. R. G.; Rubtsov, I. V. *J. Phys. Chem. A* **2005**, *109*, 10799−10802.

(26) Park, J.; Hochstrasser, R. M. *Chem. Phys.* **2006**, *323*, 78.

(27) The term co-conformation refers to the relative positions of noncovalently bonded or mechanically interlocked components with respect to each other (Fyfe, M. C. T.; Glink, P. T.; Menzer, S.; Stoddart, J. F.; White, A. J. P.; Williams, D. J. *Angew. Chem., Int. Ed. Engl.* **1997**, *36*, 2068).

(28) Kolano, C.; Helbing, J.; Kozinski, M.; Sander, W.; Hamm, P. *Nature* **2006**, *444*, 469.

(29) Larsen, O. F. A.; Bodis, P.; Buma, W. J.; Hallam, J. S.; Leigh, D. A.; Woutersen, S. *Proc. Natl. Acad. Sci. U.S.A.* **2005**, *102*, 13378.

(30) Mukamel, S. *Proc. Natl. Acad. Sci. U.S.A.* **2005**, *102*, 13717.

(31) Altieri, A.; Gatti, F. G.; Kay, E. R.; Leigh, D. A.; Martel, D.; Paolucci, F.; Slawin, A. M. Z.; Wong, J. K. Y. *J. Am. Chem. Soc.* **2003**, *125*, 8644.

(32) Hamm, P.; Kaindl, R. A.; Stenger, J. *Opt. Lett.* **2000**, *25*, 1798.

(33) Mukamel, S. *Principles of Nonlinear Optical Spectroscopy*; Oxford University Press: Oxford, U.K., 1995.

(34) Woutersen, S.; Emmerichs, U.; Bakker, H. J. *J. Chem. Phys.* **1997**, *107*, 1483.

(35) Woutersen, S.; Mu, Y.; Stock, G.; Hamm, P. *Proc. Natl. Acad. Sci. U.S.A.* **2001**, *98*, 11254.

(36) Rubtsov, I. V.; Wang, J.; Hochstrasser, R. M. *J. Chem. Phys.* **2003**, *118*, 7733.

(37) Hahn, S.; Kwak, K.; Cho, M. *J. Chem. Phys.* **2000**, *112*, 4553.

(38) Lee, C.; Park, K.-H.; Cho, M. *J. Chem. Phys.* **2006**, *125*, 114508.

(39) Hadži, D.; Bratos, S. In *The Hydrogen Bond*; Schuster, P., Zundel, G., Sandorfy, C., Eds.; Elsevier: Amsterdam, The Netherlands, 1976; Vol II, Chapter 12.

(40) Dickerson, R. E.; Drew, H. R.; Conner, B. N.; Wing, R. M.; Fratini, A. V.; Kopka, M. L. *Science* **1982**, *216*, 475.

(41) Berman, H. M.; Schneider, B. In *Nucleic Acid Structure*; Neidle, S., Ed.; Oxford University Press: Oxford, U.K., 1999; Chapter 9.

(42) Walsh, S. T. R.; Cheng, R. P.; Wright, W. W.; Alonso, D. O. V.; Daggett, V.; Vanderkooi, J. M.; DeGrado, W. F. *Protein Sci.* **2003**, *12*, 520.

(43) Rubtsov, I. V.; Kumar, K.; Hochstrasser, R. M. *Chem. Phys. Lett.* **2005**, *402*, 439.

(44) In the X-ray structure, the rotaxane is not exactly symmetric, and the angles are slightly different for the front and back NH groups, as shown in Figure 1: 102 and 125° for $\angle$(N−H,C═O_{thread}) and 8 and 16° for $\angle$(N−H,C═$O_{m.cycle}$). The values given in the text are the averages of these values.